

RESEARCH ARTICLE

Turning and multitask gait unmask gait disturbance in mild-to-moderate multiple sclerosis: Underlying specific cortical thinning and connecting fibers damage

Qingmeng Chen¹  | Takaaki Hattori¹  | Hiroshi Tomisato² | Masahiro Ohara¹ | Kosei Hirata¹ | Takanori Yokota¹ | for the Alzheimer's Disease Neuroimaging Initiative

¹Department of Neurology and Neurological Science, Graduate School of Medical and Dental Science, Tokyo Medical and Dental University, Tokyo, Japan

²Radiology Center, Division of Integrated Facilities, Tokyo Medical and Dental University Hospital, Tokyo, Japan

Correspondence

Takaaki Hattori, Department of Neurology and Neurological Science, Graduate School of Medical and Dental Sciences, Tokyo Medical and Dental University, 1-5-45, Yushima, Bunkyo-ku, Tokyo 113-8519, Japan.
Email: takaaki-hattori@umin.ac.jp

Funding information

Nakayama Foundation for Human Science; ADNI National Institutes of Health, Grant/Award Number: U01 AG024904; Department of Defense, Grant/Award Number: W81XWH-12-2-0012; National Institute on Aging; National Institute of Biomedical Imaging and Bioengineering; Canadian Institutes of Health Research

Abstract

Multiple sclerosis (MS) causes gait and cognitive impairments that are partially normalized by compensatory mechanisms. We aimed to identify the gait tasks that unmask gait disturbance and the underlying neural correlates in MS. We included 25 patients with MS (Expanded Disability Status Scale score: median 2.0, interquartile range 1.0–2.5) and 19 healthy controls. Fast-paced gait examinations with inertial measurement units were conducted, including straight or circular walking with or without cognitive/motor tasks, and the timed up and go test (TUG). Receiver operating characteristic curve analysis was performed to distinguish both groups by the gait parameters. The correlation between gait parameters and cortical thickness or fractional anisotropy values was examined by using three-dimensional T1-weighted imaging and diffusion tensor imaging, respectively (corrected $p < .05$). Total TUG duration (>6.0 s, sensitivity 88.0%, specificity 84.2%) and stride velocity during cognitive dual-task circular walking (<1.12 m/s, 84.0%, 84.2%) had the highest discriminative power of the two groups. Deterioration of these gait parameters was correlated with thinner cortical thickness in regional areas, including the left precuneus and left temporoparietal junction, overlapped with parts of the default mode network, ventral attention network, and frontoparietal network. Total TUG duration was negatively correlated with fractional anisotropy values in the deep cerebral white matter areas. Turning and multitask gait may be optimal to unveil partially compensated gait disturbance in patients with mild-to-moderate MS through dynamic balance control and multitask processing, based on the structural damage in functional networks.

Abbreviations: 3D-T1WI, three-dimensional T1-weighted imaging; ADNI, Alzheimer's Disease Neuroimaging Initiative; CC, corpus callosum; CST, corticospinal tract; DMN, default mode network; DT, dual-task; DTI, diffuse tensor image; EDSS, expanded disability status scale; FA, fractional anisotropy; FLAIR, fluid-attenuated inversion recovery; FPN, frontoparietal network; MRI, magnetic resonance imaging; MS, multiple sclerosis; ROC, receiver operating characteristic; SFG, superior frontal gyrus; SLF, superior longitudinal fasciculus; TBSS, tract-based spatial statistics; TPJ, temporo-parietal junction; TUG, timed up and go test; VAN, ventral attention network.

Data used in preparation of this article were obtained from the Alzheimer's Disease Neuroimaging Initiative (ADNI) database (adni.loni.usc.edu). As such, the investigators within the ADNI contributed to the design and implementation of ADNI and/or provided data but did not participate in analysis or writing this report. A complete listing of ADNI investigators can be found at: http://adni.loni.usc.edu/wp-content/uploads/how_to_apply/ADNI_Acknowledgement_List.pdf

This is an open access article under the terms of the [Creative Commons Attribution-NonCommercial](https://creativecommons.org/licenses/by-nc/4.0/) License, which permits use, distribution and reproduction in any medium, provided the original work is properly cited and is not used for commercial purposes.

© 2022 The Authors. *Human Brain Mapping* published by Wiley Periodicals LLC.

KEYWORDS

cognitive-motor interference, dynamic balance control, gait disturbance, multiple sclerosis, the timed up and go test

1 | INTRODUCTION

Multiple sclerosis (MS) is a chronic demyelinating, degenerative, and inflammatory disease of the central nervous system, characterized by acute attacks and sustained progression of disability (Thompson et al., 2018; Ziemssen et al., 2016). Worse long-term prognosis of MS is associated with more frequent relapses and heavier disease burden in the early phase (Brex et al., 2002; Weinschenker et al., 1991). Thus, disease-modifying therapies should be started promptly at diagnosis and optimized to minimize disease activity (Ziemssen et al., 2016).

Several assessment systems are currently used to evaluate disease activity of MS during treatment, such as the Rio score (Sormani & De Stefano, 2013), the modified Rio score (Sormani et al., 2013), and the measure of no evidence of disease activity (Rotstein et al., 2015). These assessments are based on multiple clinico-radiologic parameters, such as the number of relapses, the number of active or new lesions on magnetic resonance imaging (MRI), and/or an increase of the Expanded Disability Status Scale (EDSS) score during the past year (Rotstein et al., 2015; Sormani et al., 2013; Sormani & De Stefano, 2013). However, these assessments also have limitations; for example, the modified Rio score has low sensitivity (24%) for identifying nonresponders (Sormani et al., 2013) and the measure of no evidence of disease activity has low predictive power for long-term prognosis (Rotstein et al., 2015). The difficulty in evaluating subtle disease disability and progression will restrict these assessments to evaluate disease activity, which may be attributed in part to the cumulative effects of multifocal lesions and adaptive cortical compensatory mechanisms (Bonnet et al., 2010; Dreher & Grafman, 2003; Rotstein et al., 2015). The additional activation of the sensorimotor cortex and medial frontal regions during motor or cognitive tasks may mask the motor and cognitive impairments that occur due to ongoing neurodegeneration, even during the early stage of MS (Bonnet et al., 2010; Dreher & Grafman, 2003). Therefore, the masked disease disability will affect the assessment of clinical relapses and disease progression, leading to underestimate disease activity.

Previous studies sought to detect subtle disability in patients with MS using multitask gait and dynamic balance control (Allali et al., 2014; Brandstadter et al., 2020; Dujmovic et al., 2017; Martin et al., 2006; Spain et al., 2012). Assessment of the spatiotemporal gait parameter is one of the promising approaches to evaluate disease activity more precisely. Gait alterations arise in the absence of clinical impairments (Martin et al., 2006) and then worsen along with an increasing EDSS score (Lizrova Preiningerova et al., 2015). Multitask gait, such as performing second and third tasks during walking, is known to assess the mobility of patients with MS by inducing dual/multitask interferences (Allali et al., 2014; Dujmovic et al., 2017). To date, multitask gait has been used to differentiate phenotypes of MS (Dujmovic et al., 2017) and assess treatment response (Allali et al., 2014). Furthermore, the subtle patient-reported gait disturbance in MS only correlated with the

impaired dynamic balance control during movement, rather than gait endurance or EDSS score (Brandstadter et al., 2020). The timed up and go test (TUG) and semi-quantitative scales, such as functional gait assessment and the dynamic gait index, are widely used to evaluate dynamic balance function to maintain postural stability during movement in patients with MS (Cattaneo et al., 2014; Forsberg et al., 2017; Spain et al., 2012). TUG is an objective and simple measurement to reflect disease disability without a ceiling or floor effect, comparing with the other semi-quantitative scales (Cattaneo et al., 2014). Thus, quantitative gait analysis under walking conditions that require multitasking and turning rather than just straight walking may be more sensitive for assessing compensated gait disturbance.

The relationships between the large gray matter network and white matter tracts may account for the clinical meanings of multitask gait and turning in MS (Doi et al., 2017; Lorefice et al., 2017; Strik et al., 2021; Tripathi et al., 2019). Focal cortical atrophy, which is characterized by reduced gray matter volume and cortical thickness, is observed from the early phase of MS (Bussas et al., 2022; Eshaghi et al., 2018; Fujimori et al., 2021). Reduced cortical gray matter volume is associated with both slower velocity and higher task cost during dual/multitask walking (Doi et al., 2017; Tripathi et al., 2019) and also correlates with longer total TUG duration (Lorefice et al., 2017). As a result, multitask walking and turning may unmask subtle disability by affecting the original cortical compensatory mechanisms. In particular, cortical thickness in distinct functional networks can predict different executive task performances (Schmidt et al., 2016). Moreover, reduced gray matter correlates with connecting fibers damage (Bussas et al., 2022), while the axonal loss in the corticospinal tracts (CST) and interhemispheric sensorimotor tracts is also associated with deteriorated gait performance (Strik et al., 2021). Thus, the neural correlates of gait in cortical thickness and white matter fibers may provide essential information for evaluating disease disability in MS.

Although several studies emphasized the use of wearable sensors for multitask gait (Allali et al., 2014; Brandstadter et al., 2020), to date no comprehensive studies have directly compared multiple gait conditions in terms of unmasking the gait disturbance in patients with MS. Moreover, the neural basis of these gait conditions remains unclear. This study was conducted as a cross-sectional study to identify the tasks and gait parameters that unmask gait disturbances of patients with MS and to determine their underlying neural correlates, by using wearable sensors and brain structural MRI.

2 | MATERIALS AND METHODS

2.1 | Participants and clinical assessment

This study prospectively enrolled patients with MS treated at our institution from May 2018 to December 2020. Inclusion criteria were

(1) diagnosis of relapsing–remitting MS according to the 2017 McDonald criteria (Thompson et al., 2018); (2) age 20–59 years; and (3) right-handedness, defined by using the right hand for writing and eating with chopsticks, and not being corrected from left-handedness. Exclusion criteria were any one or more of the followings: (1) inability to walk 15 meters without assistance; (2) neurologic complications, such as epilepsy and stroke; (3) presence of other conditions that can affect gait performance, such as peripheral neuropathy and orthopedic diseases; (4) clinical improvement after acute phase treatment within 6 weeks; (5) cognitive function too poor to understand the instructions for gait examinations; (6) drug or alcohol addiction; and (7) low MRI quality due to noise, such as motion artifacts. We assessed the MS disease severity using the EDSS score (Kurtzke, 1983), and participants were then classified according to disease severity as mild (EDSS \leq 3.5) or moderate (EDSS 4.0–6.0) (Ahmad et al., 2017), in which the patients whose EDSS \leq 2.0 were defined as minimal disability (Kurtzke, 1983).

We also recruited healthy controls. Inclusion criteria were (1) normal presentations on neurologic examination; (2) age 20–59 years; (3) normal cognitive function according to the Japanese version of the Montreal Cognitive Assessment test (Nasreddine et al., 2005) and the dementia assessment sheet in the community-based Integrated Care System-21 (Awata et al., 2016); and (4) right-handedness, as previously defined. Exclusion criteria were any one or more of the following: (1) drug or alcohol addiction; (2) neurologic and psychiatric diseases, such as epilepsy and depression; and (3) low MRI quality.

In addition, we used the neuroimaging data of healthy individuals from the Alzheimer's Disease Neuroimaging Initiative (ADNI) database (2003) (<https://adni.loni.usc.edu>) to perform probabilistic tractography analysis only. Inclusion criteria were: (1) belonging to healthy control groups in ADNI who show no signs of depression, mild cognitive impairment, or dementia; (2) age 55–65 years; and (3) data available for three-dimensional T1-weighted imaging (3D-T1WI) and 54 directions diffuse tensor imaging (DTI) images scanned on 3.0 Tesla SIEMENS MRI. The exclusion criterion was low MRI quality. Demographic information and imaging data were obtained from the ADNI database. The ADNI was launched in 2003 as a public-private partnership, led by Principal Investigator Michael W. Weiner, MD. The primary goal of ADNI has been to test whether serial MRI, positron emission tomography, other biological markers, and clinical and neuropsychological assessment can be combined to measure the progression of mild cognitive impairment and early Alzheimer's disease. For up-to-date information, see www.adni-info.org.

2.2 | Standard protocol approvals, registrations, and patient consent

This study was performed in accordance with the guidelines of the Declaration of Helsinki and was approved by the Institutional Review Board of Tokyo Medical and Dental University, Faculty of Medicine. Written informed consent was obtained from all participants.

2.3 | Gait assessments

2.3.1 | Quantitative gait analysis

Spatial and temporal gait data were collected using inertial measurement units (WALK-MATE Viewer, WALK-MATE LAB., Tokyo, Japan) attached at both ankles and waist (Muto et al., 2012). Inertial measurement units included a tri-axial accelerometer with ± 8 G and a tri-axial gyroscope with ± 1000 degrees per range. All participants performed a series of fast-paced gait examinations in the hospital corridor as follows: (1) simple-task straight walking: walking a distance of 15 meters in a straight line; (2) cognitive dual-task (cognitive-DT) straight walking: straight walking while performing serial 7 s subtractions from 500; (3) motor dual-task (motor-DT) straight walking: straight walking while holding a tray with four empty plastic glasses; (4) triple-task straight walking: straight walking while performing serial 7 s subtractions from 600 and simultaneously holding a tray with four empty plastic glasses; (5) simple-task circular walking: walking along the edge of a 1-m diameter circular carpet in a clockwise direction for three laps; and (6) cognitive-DT circular walking: circular walking while performing serial 7 s subtractions from 700.

The gait parameters of gait characteristics, gait variabilities, and task cost were quantified under each walking condition. Gait characteristics included stride length, duration, and velocity. The gait variability of each gait characteristic was assessed by using the coefficient of variation, which was defined as the ratio of the standard deviation and mean. The task cost of each gait characteristic when performing additional tasks was calculated by the following formula:

$$\text{Task cost}_{\text{gait characteristic}} = \left(\text{Gait characteristic}_{\text{dual/multitask}} - \text{Gait characteristic}_{\text{simple-task}} \right) / \text{Gait characteristic}_{\text{simple-task}} \times 100\%.$$

2.3.2 | TUG test

At the end of their gait assessments, participants performed TUG three times under the standard instruction at a fast-paced rate (Kalron et al., 2017). The duration of each trial from a sitting position on a chair to sitting down on the chair was recorded. The means of durations of all trials were used as a total TUG duration for analysis.

2.4 | MRI acquisition and analyses

2.4.1 | MRI acquisition

All participants from our hospital underwent 3D-T1WI, DTI and fluid-attenuated inversion recovery (FLAIR) using a 3.0 T Scanner (MRI; MAGNETOM Spectra, Siemens Healthcare, Erlangen, Germany). The 3D-T1WI was obtained using Magnetization Prepared Rapid Gradient Echo (repetition time = 1800 ms, echo time = 2.42 ms, inversion

time = 900 ms, flip angle = 9 degrees, field of view = 250 mm × 250 mm, matrix = 256 × 256, 192 contiguous sagittal slices with 1-mm thickness). DTI was obtained using a spin-echo based single-shot echo-planar sequence (repetition time = 9500 ms, echo time = 93 ms, flip angle = 90 degrees, field of view = 240 mm × 240 mm, matrix = 80 × 80, 55 contiguous axial slices with a voxel size of 3 mm × 3 mm × 3 mm. *b*-value = 0 and 1000 s/mm², 12 directions of motion-probing gradients). FLAIR was obtained by inversion recovery T2-weighted sequence (repetition time = 10000 ms, echo time = 103 ms, inversion time = 2560 ms, flip angle = 150°, field of view = 210 mm × 196.9 mm, matrix = 384 × 180, 52 contiguous axial slices with 3-mm thickness).

The 3D-T1WI and DTI images of all normal individuals in the ADNI were obtained by a 3.0 T Scanner (MRI; MAGNETOM Prisma or Skyra, Siemens Healthcare, Erlangen, Germany). The 3D-T1WI was obtained by Magnetization Prepared Rapid Gradient Echo (repetition time = 2300 ms, echo time = 3.0 ms, inversion time = 900 ms, flip angle = 9°, matrix = 240 × 256, 192 contiguous sagittal slices with 1.0–1.2 mm thickness). DTI was obtained using a spin-echo based single-shot echo-planar sequence (repetition time = 7200 ms, echo time = 56 ms, flip angle = 90°, matrix = 1044 × 1044, 55 contiguous axial slices with a voxel size of 2 mm × 2 mm × 2 mm. *b*-value = 0 and 1000 s/mm², 54 directions of motion-probing gradients).

2.4.2 | Lesion burden: lesion segmentation toolbox

The 3D-T1WI and 2D-FLAIR were processed to generate white matter lesion masks using a lesion growth algorithm from the Lesion Segmentation Toolbox version 2.0.15 (www.statistical-modelling.de/ist.html) for Statistical Parametric Mapping 12 (Schmidt et al., 2012). The algorithm first divides the T1 images into the three main tissue classes (gray matter, white matter and cerebrospinal fluid). This information was then combined with the coregistered FLAIR intensities to calculate lesion belief maps. By using a prechosen initial threshold (κ), an initial binary lesion map was obtained, which was subsequently grown along hyperintense voxels in the FLAIR image, resulting in a lesion probability map. We manually checked the output according to the T1 images, excluded the hyperintense voxels that were out of the brain parenchyma. Finally, we generated a binary lesion mask using a threshold and then calculated the lesion volume. The optimal κ and threshold values were adopted from a previous study (Pareto et al., 2016).

2.4.3 | Cortical thickness: Qdec analysis

The 3D-T1WI images were preprocessed in the Freesurfer version 6.0 image analysis suite (<http://surfer.nmr.mgh.harvard.edu/>). We ran *recon-all* and then manually checked the output and edited the white matter and pial according to the coregistered FLAIR, which was generated for the Lesion Segmentation Toolbox. After cortical reconstruction by smoothing with a kernel of 10, cortical thickness on each vertex was generated. We conducted a whole-brain vertex-wise analysis using a general-linear model on the Freesurfer tool Qdec, and

then adjusted for age and sex. We compared cortical thickness between patients with MS and controls, and then explored the areas where cortical thickness was correlated with gait parameters or EDSS score only in patients with MS.

We displayed the results of Qdec analysis on fsaverage inflated surfaces, and identified the anatomic names of the cortex and the functional networks by comparing with the Desikan–Killiany atlas (Desikan et al., 2006) and the 7Networks atlas (Yeo et al., 2011), respectively. The 7Networks is an atlas of seven functional networks obtained from resting-state functional MRI data from 1000 individuals (Yeo et al., 2011).

2.4.4 | White matter: tract-based spatial statistics analysis

Image processing and voxel-wise statistics analysis of all DTI images were performed using the FMRIB Software Library (FSL) version 6.0 (www.fmrib.ox.ac.uk/fsl; Analysis Group, FMRIB, Oxford, UK) on a macOS system (Smith et al., 2004). Eddy current-induced distortions and motion were corrected by using the tool eddy 6.0.1 (Andersson & Sotiropoulos, 2016). Individual participant fractional anisotropy (FA) maps were created by fitting diffusion tensors on corrected data using the FMRIB Diffusion Toolbox. Finally, tract-based spatial statistics (TBSS) analysis was performed (Smith et al., 2006). In summary, all FA data for individual participants were aligned into a common space, and the centers of all tracts common to the group were represented as a thinned mean FA skeleton that was set as a threshold at 0.2. The TBSS projected an individual participant's aligned FA data onto this skeleton and fed the results into voxel-wise statistics models. The permutation-based inference tool “randomize” was used for statistical analysis, and permutation was set at 5000. The FA maps were compared between patients with MS and controls using nonparametric two-sample *t* tests. We performed a correlation analysis to explore the correlations between FA values and gait parameters or EDSS score only in patients with MS. All statistical analyses were adjusted for age and sex. We identified the anatomic names of the white matter tracts by comparing with the JHU DTI-based white-matter tractography atlas (Hua et al., 2008).

2.4.5 | Probabilistic tractography analysis

To visualize the neural correlates for the impaired gait in patients with MS, we reconstructed tractographies connecting gait-related cortical areas and white matter regions by probabilistic tractography analysis. However, we used 3D-T1 and DTI data in the ADNI database instead of our data because of the limited diffuse directions of our DTI data. Preprocessing all imaging data was performed by using Freesurfer and FSL. Probabilistic tractography analysis was performed by using tool *probrackX* in the FMRIB Diffusion Toolbox (Behrens et al., 2003, 2007). We created a seed mask by transforming the gait-related cortical areas resulting from Qdec analysis into the individual participant's cortical surfaces, and then converting it as a binary mask. We also

created a waypoint mask by projecting the gait-related white matter areas resulting from the TBSS analysis back to the individual participant's native space, and then converting it as a binary mask. Probabilistic fiber tracking was initiated from all voxels within the seed mask to generate 5000 streamline samples with a curvature threshold of 0.2. Probabilistic tractography analysis was performed by using the approach of a single mask model with a seed mask and a waypoint mask when both Qdec and TBSS analysis identified the areas with statistical significance. However, in another approach, a multiple masks model was used when Qdec identified several cortical areas with statistical significance, in which multiple tractographies were generated from multiple seed masks. The generated tractographies for each participant were spatially normalized to MNI 152 standard-space. Finally, the mean tractography was created by summing all participants and then averaging the results.

2.5 | Statistical analysis

The normality of data was evaluated by the Kolmogorov–Smirnov test. We performed intergroup comparisons using the Mann–Whitney *U* test for quantitative variables because of the limited sample size and chi-square test for qualitative variables. Mean difference (patients minus controls) was calculated using *t* test. Effect sizes of gait parameters were evaluated by *r* for the Mann–Whitney *U* test, and the phi coefficient for the chi-square test, respectively.

The gait parameters with the largest effect size for the intergroup difference under each condition were sequentially fed into a receiver operating characteristic (ROC) analysis to evaluate classification efficacy to discriminate patients with MS from controls. The optimal cut-

offs were identified as the points with the minimum distance to the best point (100% sensitivity and 100% specificity). Then, we used the determined optimal cut-off values to divide patients with MS and controls in a binary model as positive and negative groups. The effect sizes and odds ratios obtained from the chi-square test were used to evaluate classification efficacy.

The relationships between those gait parameters and EDSS scores were explored using a partial correlation analysis adjusted for age and sex. The statistical significance was defined by *p*-values of <.05. All statistical analyses were processed on the statistical software Statistical Package for Social Sciences (SPSS) version 28.0 (SPSS for Macintosh, IBM Corp, Armonk, NY, USA).

For Qdec analysis, the statistical significance was defined as the corrected *p*-value of <.05 after multiple comparisons using Monte Carlo correction. The uncorrected *p*-value of <.005 was used as a criterion to show a trend.

For TBSS analysis, statistical significance was defined by the threshold-free cluster enhancement corrected *p*-value of <.05.

3 | RESULTS

This study recruited 29 patients with MS, however, 4 patients were excluded for the following reasons: one patient refused gait examinations, one patient refused to perform cognitive tasks during walking, one patient was unable to maintain balance when performing a motor task during straight walking, and MRI quality for one patient was poor due to motion. Thus, 25 patients with MS and 19 age- and sex-matched controls were included in the analyses (Table 1). Age, total TUG duration, gait characteristics, and task costs were in a normal

TABLE 1 General characteristics of patients with MS and healthy controls

	Patients with MS (<i>n</i> = 25)	Healthy controls (<i>n</i> = 19)	<i>p</i> value
Age (mean ± SD), years	45.9 ± 8.2	42.2 ± 11.3	.207
Female, <i>n</i> (%)	19 (76.0)	10 (52.6)	.123
Disease duration (mean ± SD), years	9.9 ± 7.6	-	-
EDSS score, median (IQR)	2.0 (1.0–2.5)	-	-
Minimal severity (EDSS ≤2.0), <i>n</i> (%)	18 (72.0)	-	-
Mild severity (EDSS ≤3.5), <i>n</i> (%)	21 (84)	-	-
Moderate severity (EDSS 4.0–6.0), <i>n</i> (%)	4 (16)	-	-
Functional system score in mental functions, median (IQR)	0.0 (0.0–1.0)	-	-
Under treatments on examination, <i>n</i> (%)	16 (64.0) ^a	-	-
Disease modified therapies, <i>n</i> (%)	14 (56.0) ^a	-	-
Interferon beta-1a, <i>n</i> (%)	4 (16.0)	-	-
Glatiramer acetate, <i>n</i> (%)	3 (12.0)	-	-
Dimethyl fumarate, <i>n</i> (%)	3 (12.0)	-	-
Fingolimod, <i>n</i> (%)	4 (16.0) ^a	-	-
Low-dose corticosteroids, <i>n</i> (%)	3 (12.0) ^a	-	-

Abbreviations: EDSS, Expanded Disability Status Scale; IQR, interquartile range; MS, multiple sclerosis; SD, standard deviation.

^aOne patient with multiple sclerosis received a combination therapy with fingolimod and low-dose corticosteroids.

distribution, whereas gait variabilities and EDSS scores did not show normal distribution. The minimal disability EDSS was ≤ 2.0 in 72% of patients with MS, and 64% of patients were under treatment when undergoing examinations (Table 1).

3.1 | Gait parameters between patients with MS and controls

Total TUG duration was longer in patients with MS than in controls (effect size -0.670 , $p < .001$), as shown in Table 2. The gait characteristics in patients were worse than the gait characteristics in healthy controls to a varying extent depending on different walking conditions (effect size -0.630 to -0.338 , $p < .001$ to $p = .025$; Table 2). Worsened gait characteristics were accompanied by heavier task costs (effect size -0.466 to -0.023 , $p = .002$ to $.888$; Table S1) and larger gait variabilities (effect size -0.427 to -0.052 , $p = .004$ to $.752$; Table S2). The stride velocity showed the largest intergroup difference than differences in other gait parameters under the same condition, including stride length and duration, gait variabilities and task costs, as

presented in Table 2 and Tables S1 and S2. Compared to other walking conditions, the stride velocity under cognitive-DT circular walking showed the largest intergroup difference between patient with MS and controls (0.87 ± 0.28 vs. 1.28 ± 0.21 , effect size -0.630 , $p < .001$; Table 2), and the highest intergroup difference of task cost as well ($-50.0\% \pm 13.1\%$ vs. $-37.6\% \pm 8.4\%$, effect size -0.459 , $p < .001$; Table S1). A subgroup analysis for patients with MS with minimal disability and controls also showed similar results (Tables S3–S5).

3.2 | ROC analysis

An ROC analysis demonstrated that total TUG duration (cut-off >6.00 seconds, sensitivity 88.0%, specificity 84.2%, effect size 0.722, odds ratio 39.111) and the stride velocity during cognitive-DT circular walking (<1.12 m/s, sensitivity 84.0%, specificity 84.2%, effect size 0.679, odds ratio 28.000) had higher effect sizes and odds ratios than those of other parameters to differentiate patients with MS from controls, as shown in Table 3. The two gait parameters (both effect size 0.675, odds ratio 26.667) also had the highest effect size and odd

TABLE 2 Quantitative gait parameters of patients with MS and healthy controls

	Patients with MS (n = 25)	Healthy controls (n = 19)	Mean difference	Effect size (r)	p value
Total TUG duration, s	7.36 \pm 1.50	5.53 \pm 0.60	1.83	-0.670	<.001
Simple-task straight walking					
Stride length, m	1.51 \pm 0.27	1.66 \pm 0.11	-0.15	-0.395	.009
Stride duration, s	0.88 \pm 0.10	0.81 \pm 0.08	0.07	-0.359	.017
Stride velocity, m/s	1.75 \pm 0.41	2.05 \pm 0.20	-0.30	-0.448	.002
Cognitive dual-task straight walking					
Stride length, m	1.33 \pm 0.29	1.55 \pm 0.19	-0.21	-0.430	.004
Stride duration, s	1.10 \pm 0.35	0.87 \pm 0.14	0.23	-0.423	.004
Stride velocity, m/s	1.33 \pm 0.47	1.83 \pm 0.39	-0.50	-0.509	<.001
Motor dual-task straight walking					
Stride length, m	1.32 \pm 0.23	1.51 \pm 0.13	-0.19	-0.470	.001
Stride duration, s	0.91 \pm 0.13	0.84 \pm 0.08	0.07	-0.338	.025
Stride velocity, m/s	1.47 \pm 0.31	1.82 \pm 0.19	-0.46	-0.559	<.001
Triple-task straight walking					
Stride length, m	1.23 \pm 0.25	1.46 \pm 0.13	-0.23	-0.502	.001
Stride duration, s	1.06 \pm 0.25	0.88 \pm 0.11	0.18	-0.455	.002
Stride velocity, m/s	1.23 \pm 0.36	1.69 \pm 0.24	-0.46	-0.623	<.001
Simple-task circular walking					
Stride length, m	0.91 \pm 0.15	1.06 \pm 0.10	-0.15	-0.498	.001
Stride duration, s	0.94 \pm 0.19	0.81 \pm 0.11	0.13	-0.409	.006
Stride velocity, m/s	1.00 \pm 0.25	1.32 \pm 0.19	-0.32	-0.559	<.001
Cognitive dual-task circular walking					
Stride length, m	0.89 \pm 0.16	1.06 \pm 0.10	-0.17	-0.509	<.001
Stride duration, s	1.10 \pm 0.28	0.84 \pm 0.13	0.26	-0.570	<.001
Stride velocity, m/s	0.87 \pm 0.28	1.28 \pm 0.21	-0.41	-0.630	<.001

Note: All data were presented as mean \pm SD. See other abbreviations in Table 1 legend.
Abbreviation: TUG, timed up and go test.

TABLE 3 The classification efficacy of gait parameters to discriminate patients with MS and healthy controls

Gait parameters	Cut off	Sensitivity (%)	Specificity (%)	Area under the curve	Effect size (ϕ)	Odds ratio (MS/controls)
Total TUG duration, s	>6.00	88.0	84.2	0.895	0.722	39.111
Stride velocity under each condition, m/s						
Simple-task straight walking	<1.91	76.0	73.7	0.764	0.494	8.867
Cognitive dual-task straight walking	<1.57	72.0	78.9	0.800	0.505	9.643
Motor dual-task straight walking	<1.68	72.0	78.9	0.829	0.505	9.643
Triple-task straight walking	<1.64	92.0	68.4	0.867	0.542	15.813
Simple-task circular walking	<1.20	76.0	78.9	0.829	0.545	11.875
Cognitive dual-task circular walking	<1.12	84.0	84.2	0.872	0.679	28.000

Note: See abbreviations in Table 1 legend.

ratio than those of other parameters to differentiate patients with MS with minimal disability from controls (Table S6).

3.3 | Correlations between EDSS and gait parameters

A partial correlation analysis showed that longer total TUG duration (correlation coefficient 0.589, $p = .003$) and slower stride velocity during all walking conditions besides triple-task straight walking (correlation coefficient -0.568 to -0.419 , $p = .005$ to $.047$) were associated with higher EDSS score, as presented in Table S7.

3.4 | Intergroup comparison for cortical thickness or FA maps

The lesion volume of patients with MS was 6.81 ± 7.99 ml, with a median of 4.90 and an interquartile range of 1.06 and 10.18 ml. The cortical thickness tended to be thinner in the bilateral precuneus, left caudal anterior cingulate cortex, bilateral superior frontal gyrus (SFG), and left medial SFG in patients with MS than in controls (uncorrected $p < .05$, Figure 1a). The FA values significantly decreased in the corpus callosum (CC), bilateral CST, bilateral superior longitudinal fasciculus (SLF), and other tracts in patients with MS compared with controls (corrected $p < .05$, Figure 1b). Moreover, TBSS analysis showed that higher EDSS scores were correlated with lower FA values in the CC and bilateral white matter tracts, such as CST and SLF, in patients with MS (corrected $p < .05$, Figure 1c).

3.5 | Neuroimaging for total TUG duration

Total TUG duration was negatively correlated with cortical thickness in the left precuneus and left temporoparietal junction (TPJ). The correlated areas belonged to parts of the functional networks in the left hemisphere as follows: (1) the inferior parietal lobule, precuneus, and

isthmus of the cingulate gyrus—the default mode network (DMN); (2) banks of the superior temporal sulcus (STS)—the ventral attention network (VAN); and (3) the precuneus, isthmus of the cingulate gyrus, and lingual gyrus—the visual network (corrected $p < .05$). Figure 2a,b showed these structures, and the coordinates and anatomies of them were shown in Table S8. Lower FA values in CC, the cingulum, bilateral CST, and bilateral SLF were correlated with longer total TUG duration (corrected $p < .05$), as shown in Figure 2c with the coordinates and anatomies presented in Table S9.

Participants enrolled from the ADNI database were 11 healthy control individuals (3 males, 8 females; age 60.8 ± 3.2 years). Tractography analysis with the single mask model reconstructed the following tractographies: (1) the lateral long association fibers, including SLF, connecting the left TPJ with the left prefrontal lobe (Figure 3a, blue); and (2) the medial long association fibers, including the cingulum, connecting the left precuneus with left medial prefrontal lobe and temporal and parietal lobes (Figure 3b,d, green). The lateral long association fibers (Figure 3d, blue) mainly projected to the DMN and VAN. The medial long association fibers (Figure 3d, green) mainly projected to the DMN, VAN, and FPN. Tractography analysis with the multiple masks model reconstructed the short association fibers connecting the left TPJ with the left precuneus and adjacent areas (Figure 3c,d, black), and projecting to the DMN.

3.6 | Neuroimaging for stride velocity during cognitive-DT circular walking

Slower stride velocity during cognitive-DT circular walking was correlated with thinner cortical thickness in the left precuneus and left TPJ as well (corrected $p < .05$), presented in Figure 4a and Table S8. The correlated areas belonged to parts of the functional networks as follows: (1) the left precuneus and left inferior parietal lobule—the DMN; (2) the banks of the left STS and parts of the left cingulate cortex—the VAN; (3) the left medial SFG—the FPN; and (4) the right postcentral cortex—the sensorimotor network (Figure 4b). The FA values were not correlated with the stride velocity during cognitive-DT circular walking.

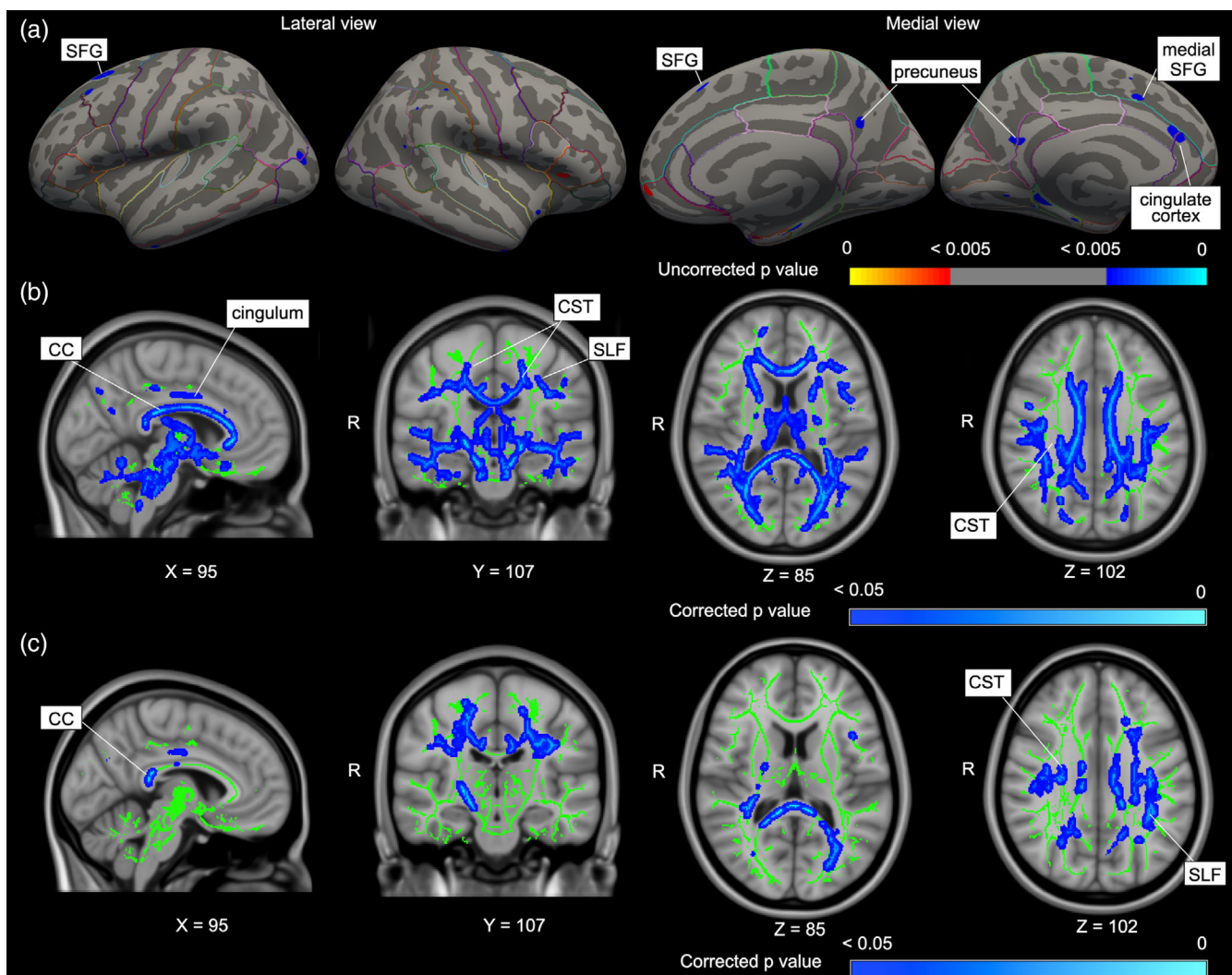


FIGURE 1 Structural alterations between both groups and correlated areas with EDSS score in patients with MS. (a) Areas where cortical thickness tends to be larger (red) or smaller (blue) in patients with MS than controls are shown (uncorrected $p < .05$). (b) Areas where FA values are significantly lower (blue) in patients with MS than controls are shown (corrected $p < .05$). (c) Regions where lower FA values are correlated with higher EDSS score in patients with MS (corrected $p < .05$). CC, corpus callosum; EDSS, expanded disability status scale; FA, fractional anisotropy; MS, multiple sclerosis; SFG, superior frontal gyrus; SLF, superior longitudinal fasciculus

Tractography analysis with the multiple masks model reconstructed the following tractographies: (1) the long association fibers, including the cingulum, connecting the left precuneus with the left medial SFG and left cingulate cortex (Figure 4c,d, green); (2) the inter-hemispheric fibers connecting the left precuneus with the right post-central gyrus (Figure 4c,d, yellow); and (3) the short association fibers connecting the left precuneus with left TPJ (Figure 4c,d, black). The long association fibers (Figure 4d, green) projected to the DMN, VAN, and FPN. The short association fibers (Figure 4d, black) projected to the DMN.

4 | DISCUSSION

This study showed that total TUG duration and the stride velocity during cognitive-DT circular walking had the highest discrimination

efficacy between patients with MS and controls. Regional atrophy in the left precuneus and left TPJ and white matter damage were associated with the deterioration of both gait parameters, which may involve the impaired function of DMN, VAN, and FPN.

4.1 | Dual/multitask interference and dynamic balance challenging for MS

The results of ROC analysis showed that dual-task interference induced by cognitive-DT walking and additional dynamic balance control required for turning are helpful to detect subtle gait disturbance that can distinguish patients with MS from controls, especially for patients with MS with minimal disability.

The dual/triple-task is the typical attention-demanding task. According to a central capacity sharing model (Tombu &

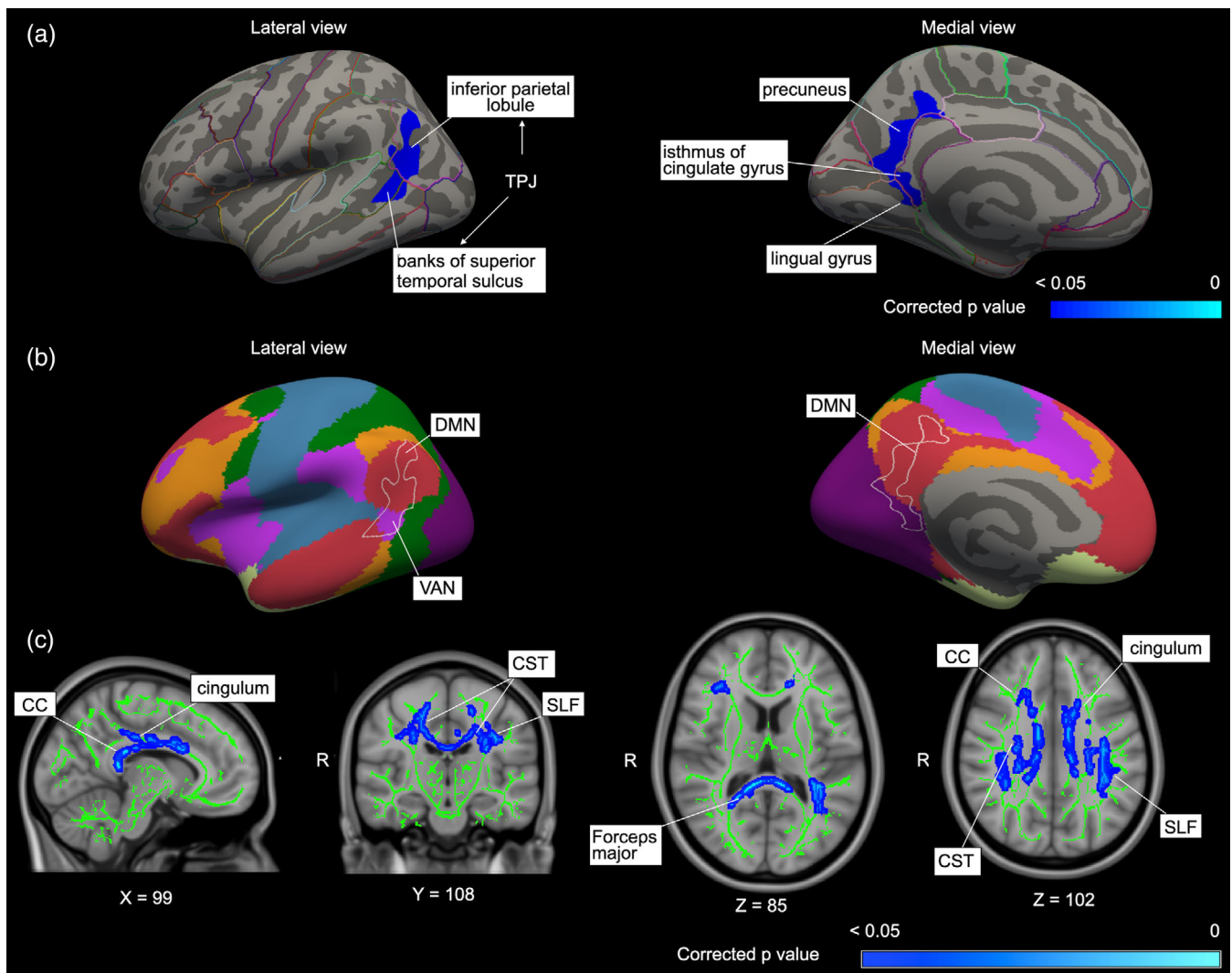


FIGURE 2 Correlated areas with total TUG duration in patients with MS. (a) Areas where thinner cortical thickness is correlated with longer total TUG duration (corrected $p < .05$, shown by blue). TPJ includes the inferior parietal lobule and banks of the superior temporal sulcus. (b) Outline of the correlated areas is shown by a white line and projected on the functional networks atlas 7Networks. The correlated areas are located on parts of the DMN (red) and VAN (violet). (c) Areas where lower FA values are associated with longer total TUG duration (corrected $p < .05$, shown by blue). DMN, default mode network; TPJ, temporoparietal junction; TUG, timed up and go test; VAN, ventral attention network. See other abbreviations in Figure 1 legend

Jolicoeur, 2003) and a bottle-neck model (Logie et al., 2004), the overloaded attentional demands and necessity to allocate attention for concurrent tasks often cause interferences among the brain resources, leading to decompensated performance of the task or tasks, especially in multitask execution. Our study finds that the differences in gait characteristics and variabilities between patients with MS and controls increased when adding the task(s) to the simple-task walking, accompanied by heavier task costs. This finding is consistent with those of previous studies, which showed decreased gait velocity and increased gait variabilities in patients with MS performing dual/multitask gait (Allali et al., 2014; Dujmovic et al., 2017). The higher dual-task cost of stride velocity was associated with the atrophy in gray matter and worse cognitive function; (Tripathi et al., 2019) whereas, similar deterioration of performance was observed in a

previous research under the conditions of increasing or fixed-demand dual tasks (Hamilton et al., 2009). Thus, reduced attentional capacity (Tripathi et al., 2019) and impaired attentional allocation (Hamilton et al., 2009) may enable interferences to unmask the partially compensated gait disturbances in patients with MS.

The present study also demonstrated that effect sizes of the intergroup differences in total TUG duration and gait characteristics under the simple-task circular walking were larger than those of gait parameters under the simple-task straight walking. Because a previous investigation found that impaired postural balance only correlates with TUG and the fastest safe walking speed (Brincks et al., 2017), additional dynamic balance control for turning may account for our findings. Dynamic balance control necessitates extra cortical functions in addition to those used for straight walking, such as integrating

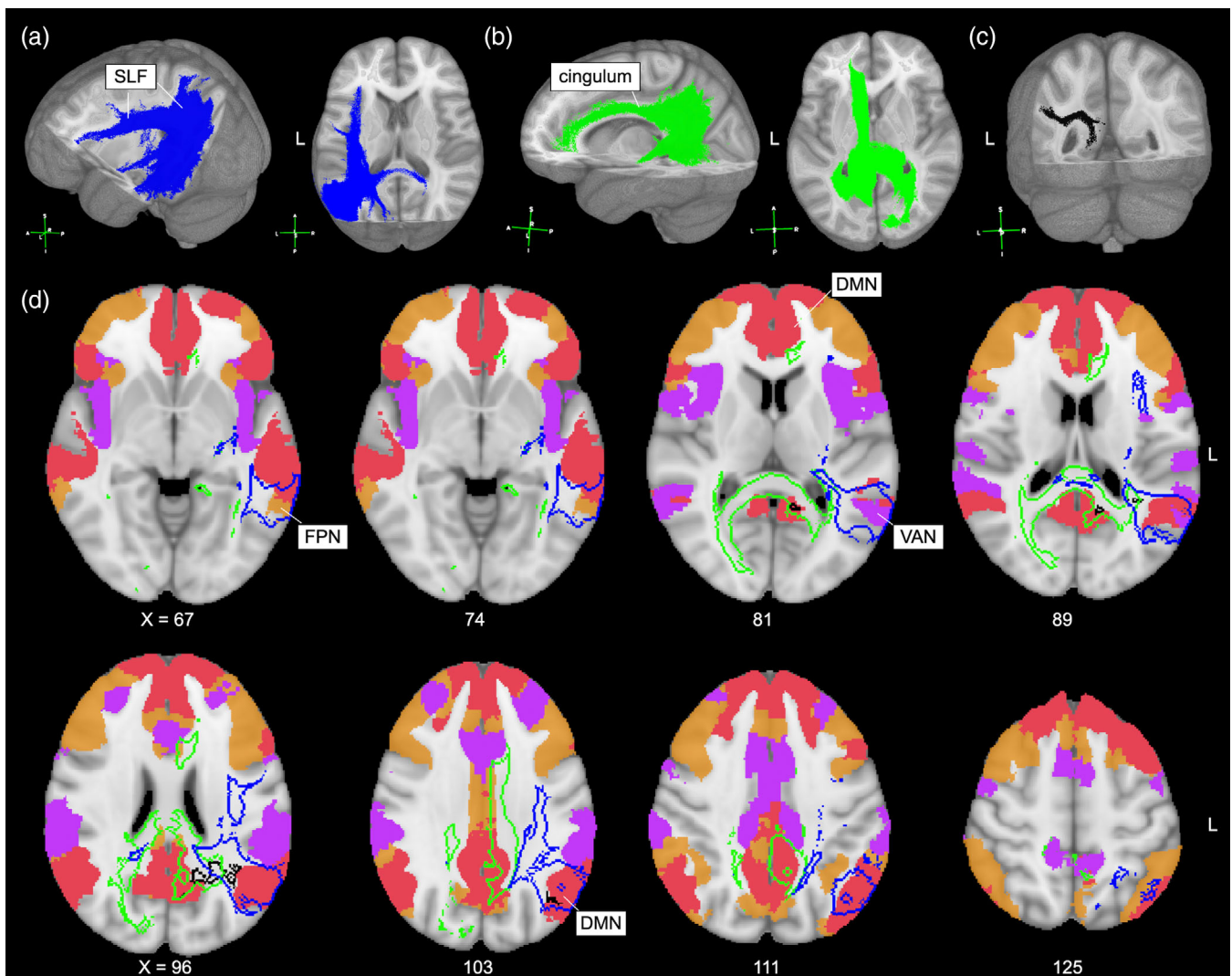


FIGURE 3 Tractographies reconstructed from correlated areas with total TUG duration. (a) Tractography that projects from left TPJ (Figure 2a) and passes through the white matter areas where TBSS analysis identified (Figure 2c) (blue). Display threshold is 1000. (b) Tractography that projects from the left precuneus and adjacent areas (Figure 2a) and passes through the white matter areas where TBSS analysis identified (Figure 2c) (green). Display threshold is 1000. (c) Tractography which connects left TPJ (Figure 2a) with the left precuneus and adjacent areas (Figure 2a) (black). Display threshold is 100. (d) Outlines of reconstructed tractographies (blue, green, and black, defined in A–C) are shown on the functional network atlas 7Networks. Reconstructed tractographies overlap the DMN (red), FPN (orange) and VAN (violet). FPN, frontoparietal network; TBSS, tract-based spatial statistics. See other abbreviations in Figures 1 and 2 legends

multisensory information, achieving purposeful movements and postural adjustment (Lorefice et al., 2017; Takakusaki, 2017). Thus, tasks that require dynamic balance control may unmask their brain dysfunction because our patients with MS had widespread microstructural damage in the white matter, and tended to be thinner in regional cortical areas such as SFG and precuneus.

Considered together, multitask processing and turning are complex tasks that require additional brain resources. Specifically, TUG can be used to assess dynamic balance and gait functions according to a serial of continuous and different movements, whereas cognitive-DT circular walking can reflect dynamic balance and cognitive functions. Moreover, although diffuse tissue damage-dependent recruitment of medial prefrontal regions occurs in patients with MS

for preserving good cognitive performance, this recruitment will collapse under the most complex cognitive task (Bonnet et al., 2010). Therefore, these complex gait conditions may lead to numerous brain resources demands, resulting in functional decompensation, then consequently unmasking the gait disturbance.

4.2 | Neural correlates of complex gait conditions

The study findings showed that prolonged TUG duration correlates with regionally cortical thinning in the left precuneus and in the left TPJ and with widespread white matter tract damage involving CC, cingulum, CST, and SLF, whereas cognitive-DT circular walking only

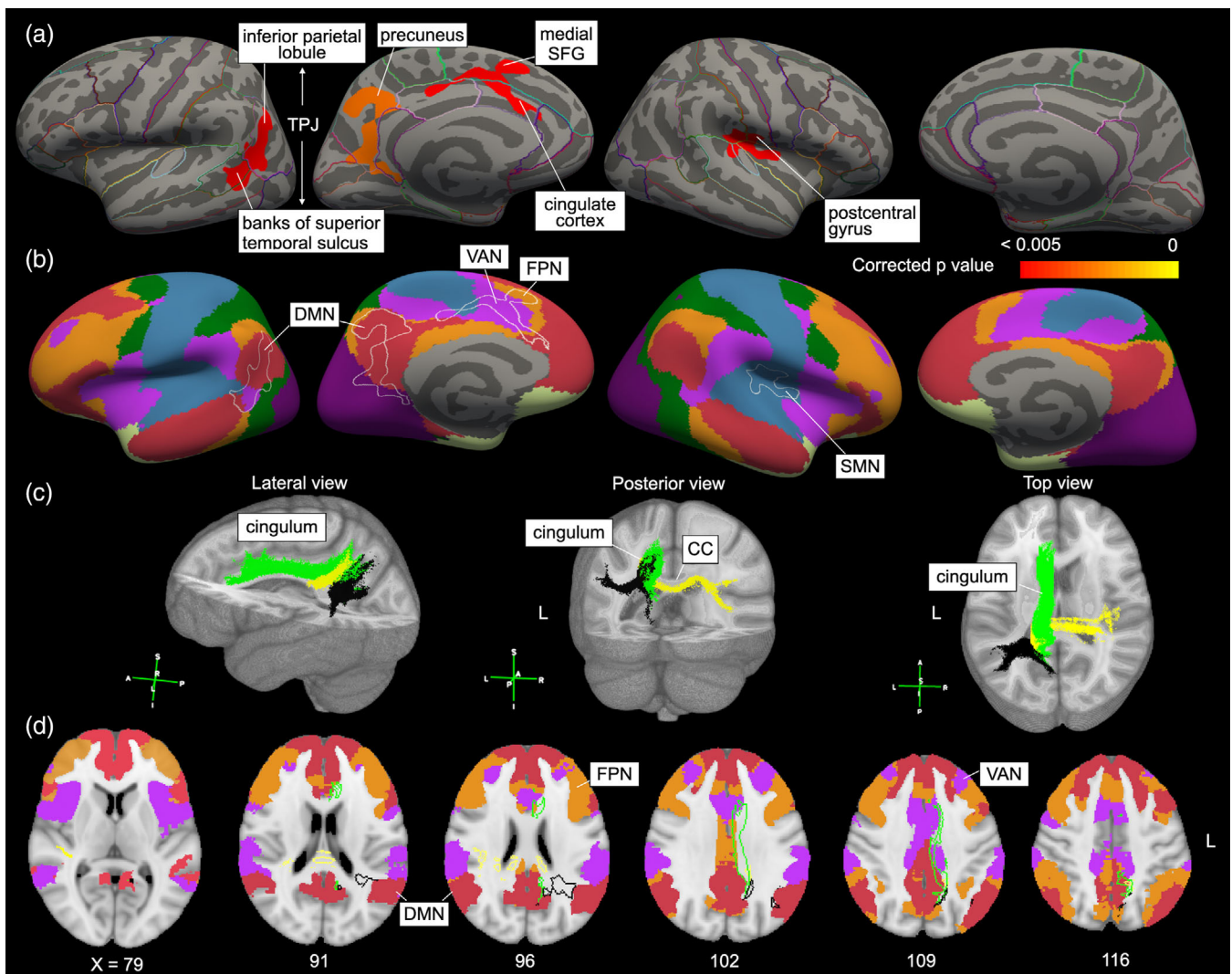


FIGURE 4 Correlated areas for stride velocity during cognitive-DT circular walking and reconstructed tractographies. (a) Areas where smaller cortical thickness is correlated to slower stride velocity during cognitive-DT circular walking (corrected $p < .05$, shown by red/yellow). (b) Outlines of the identified areas are projected on the functional network atlas 7Networks (shown by white line). (c) Tractographies connecting those cortical areas are reconstructed. They connect between the left precuneus and the left medial SFG and left cingulate cortex (green), between the left precuneus and the right postcentral gyrus (yellow) and between the left precuneus and the left TPJ (black). Display thresholds are 500 (green), 200 (yellow) and 20 (black) for each tract. (d) Outlines of reconstructed tractographies (green, yellow and black), defined in (d) are shown on the functional network atlas 7Networks. Reconstructed tractographies overlap the DMN (red), FPN (orange), and VAN (violet). DT, dual-task; SMN, sensorimotor network. See other abbreviations in Figures 1–3 legends

correlates with cortical thickness of widespread regions, including the left precuneus and left TPJ. However, both of these assessments necessitate functions of DMN, VAN, and FPN. Therefore, reduced cortical thickness in specific areas may result in dysfunction of the corresponding functional networks, coincident to previous study (Schmidt et al., 2016).

4.2.1 | Precuneus and DMN

Based on the results of this study, we speculate that the left precuneus plays a central role in dynamic balance control and multitask processing because of its connections to medial frontal lobes, left TPJ,

and right postcentral gyrus, all of which are involved in TUG and/or cognitive-DT circular walking. This interaction coincides with the anatomic characteristics of the precuneus, which has strong structural connections with broad brain areas, such as connecting to the frontal and temporal lobes by the cingulum, as well as the superior temporal gyrus by the middle longitudinal fasciculus (Tanglay et al., 2022).

In terms of dynamic balance control, the precuneus affects spatial memory and spatial updating (Blumen et al., 2014; Gonzales et al., 2019; Jahn et al., 2012), which is the only brain area that produces load-dependent activation when an individual is tracking the positions of objects that move out of view (Jahn et al., 2012). Furthermore, the activation in the precuneus while performing a spatial task is positively associated with speed in fast-paced walking (Gonzales

et al., 2019). Turning during TUG and circular walking result in the surrounding circumstances changing such that patients with MS must maintain an awareness of the locations so they know where to go next. Therefore, the left precuneus may be involved in updating spatial representations when turning, which is important for dynamic balance control.

In terms of multitask processing, the precuneus has been observed to be engaged in cognitive processing during dual-task walking (Blumen et al., 2014; Doi et al., 2017; Tripathi et al., 2019). Several structural studies showed that lower gray matter volume in the precuneus is correlated with higher dual-task cost (Tripathi et al., 2019) and slower dual-task walking speed (Doi et al., 2017). Furthermore, the precuneus is activated when performing imagery walking tasks, which is also associated with behavior performance during actual dual-task walking (Blumen et al., 2014). The activation in the precuneus increases in response to cognitive demands, especially during imagined walking-while-talking. Thus, the left precuneus may also be involved in cognitive processing when performing cognitive-DT circular walking.

In terms of the DMN, the precuneus is seen as a core hub of the DMN (Utevsky et al., 2014). The DMN was originally defined by the areas that are deactivated while performing goal-directed activities and that are activated at rest (Raichle et al., 2001). However, recent research has shown that the left precuneus is functionally coupled with left FPN in goal-directed cognition under an autobiographical planning task (O'Connell & Basak, 2018). Moreover, the DMN is more often coupled with attentional networks during a complex cognitive task than a simple cognitive task (O'Connell & Basak, 2018). These findings support our results of probabilistic tractography analysis for both complex gait conditions.

Based on these understandings, the left precuneus may engage in TUG and cognitive-DT circular walking from both structural and functional aspects.

4.2.2 | TPJ and VAN

The left inferior parietal lobule and left posterior STS correlates with TUG and cognitive-DT circular walking performance in our study, as parts of the left TPJ. The posterior STS tends to be strongly coactivated with the inferior parietal lobule in the same hemisphere (Erickson et al., 2017), whereas the damaged left posterior STS will lead to dysfunction of right posterior STS (Sliwinska et al., 2020). Thus, the left posterior STS plays an important role in integrating functions of the bilateral TPJ. The TPJ bilaterally connects to VAN (Kucyi et al., 2012), which is activated by bottom-up behaviorally relevant signals, and it then interacts with the dorsal attention network to reorient attention when salient or unexpected sensory stimuli occur (Corbetta & Shulman, 2002). During TUG and cognitive-DT circular walking, participants must be alert to changing circumstances to reorient attention when unexpected events occur. Therefore, the cortical atrophy in left TPJ may result in dysfunctions of bilateral VAN, leading to impaired attentional reorientation during turning.

4.2.3 | Medial frontal lobe and FPN

An interesting finding in our study is that the medial frontal lobe engages directly in cognitive-DT circular walking and indirectly in TUG through a precuneus-cingulum-medial frontal lobe neural network (Tanglay et al., 2022). The gray matter volume in medial frontal lobe, such as the medial SFG and anterior cingulate cortex, is associated with dual-task walking speed and dual-task cost (Doi et al., 2017; Tripathi et al., 2019). Furthermore, the left medial SFG and anterior cingulate cortex are functionally activated when performing the dual tasks simultaneously versus performing each task separately (Dreher & Grafman, 2003). The functional networks to which they belong may account for these correlations. The left medial SFG is part of the FPN, which plays a key role in controlling a volitional goal-driven behavior (Marek & Dosenbach, 2018). The left anterior cingulate cortex is part of both the VAN and FPN. Therefore, cortical thinning in the left medial frontal lobe may result in impairments in task execution and attention reorientation, leading to deteriorated gait performance during complex gait conditions.

4.2.4 | Unique neural correlates underlying each condition

Widespread microstructural damage among the splenium and body of CC, CST, and SLF is only associated with total TUG duration in patients with MS. The splenium of CC connects the bilateral parietal, temporal, and occipital lobes (Hofer & Frahm, 2006) affecting multi-sensory integration and directional orientation (Ino et al., 2008), whereas the body of CC connects the bilateral frontal lobes (Hofer & Frahm, 2006) affecting feedforward postural motor learning (Peterson et al., 2017). Patients with MS who exhibit poorer integrity of the CC experience more difficulty in improving dynamic balance control during repeated balance training (Peterson et al., 2017). The CST may be damaged by focal lesions in MS, resulting in sensory-motor disability (Fritz et al., 2015). The TUG is a measure of gait and balance; thus, it correlates with the integrity of the CC and CST. Moreover, our study found that SLF is involved in TUG by connecting the TPJ to the inferior frontal lobe. Because the SLF serves as the connecting fibers of the VAN (Hattori et al., 2018), damage in the SLF will lead to limiting attentional reorientation, thereby restricting TUG performance.

Contrary to TUG, cognitive-DT circular walking correlates with the right postcentral cortex rather than white matter tracts. Previous work demonstrated that a widespread right sensorimotor network is recruited to compensate the injury of left CST (Rocca et al., 2004). Motor load in cognitive-DT circular walking may be partly counteracted by cognitive-motor interference, compared with that in TUG. Therefore, the sensorimotor network may be able to compensate for the sensory-motor disability by CST, so that the cortical thickness in right postcentral cortex is associated with the stride velocity under cognitive-DT circular walking.

4.3 | Complex gait conditions and pathological changes in early disease

The precuneus is known to be the first region that will become atrophic in patients with MS (Eshaghi et al., 2018), secondarily degenerated due to the white matter and cortical damage (Haider et al., 2016). This study also showed a trend of reduced cortical thickness in the precuneus in patients with MS. Considered together, we speculate that these complex gait conditions can unveil early and subtle disability underlying reduced cortical thickness in the precuneus.

This study has several limitations. First, the design is a cross-sectional study, and a longitudinal study is needed to elucidate the associations between gait parameters and structural degeneration of relevant networks during disease progression in the same individuals. Second, although we found common neural networks involved in complex gait conditions as parts of the DMN, VAN, and FPN, we determined this commonality by using structural images and diffusion images in the ADNI database because our DTI data had only a limited number of directions. We also did not evaluate their functions. A future study is warranted to evaluate the association between functions of the DMN, VAN, and FPN using functional MRI and gait disturbance. Finally, due to the limited sample size, we only adjusted for age and sex when conducting statistical analyses.

In conclusion, these results suggest that patients with MS have impaired dynamic balance control and multitask processing correlating with regional cortical thinning and microstructural damage in major white matter tracts, involving the functions of the DMN, VAN, and FPN. Total TUG duration and stride velocity during cognitive-DT circular walking are sensitive measures to evaluate gait disturbances in MS. In a future study, these tasks may be used for early diagnosis or monitoring of disease activity of MS.

AUTHOR CONTRIBUTIONS

Qingmeng Chen, MD: design and conceptualization of the study, data acquisition, interpretation, data analysis, and drafting the manuscript. **Takaaki Hattori**, MD, PhD: design and conceptualization of the study, data acquisition, interpretation, and drafting the manuscript. **Hiroshi Tomisato**: data acquisition. **Masahiro Ohara**, MD: data acquisition and interpretation. **Kosei Hirata**, MD, PhD: data acquisition. **Takanori Yokota**, MD, PhD: clinical practice supervision.

ACKNOWLEDGMENTS

The authors thank Kina Satoko M.D. and clinical staffs at the Tokyo Medical and Dental University Hospital for taking care of patients and Devera G. Schoenberg, M.Sc., Editor for editing the manuscript. Data collection and sharing for this project were funded by ADNI (National Institutes of Health Grant U01 AG024904) and DOD ADNI (Department of Defense award number W81XWH-12-2-0012). ADNI is funded by the National Institute on Aging, the National Institute of Biomedical Imaging and Bioengineering, and through generous contributions from the following: AbbVie, Alzheimer's Association; Alzheimer's Drug Discovery Foundation; Araclon Biotech; BioClinica, Inc.; Biogen; Bristol-Myers Squibb Company; CereSpir, Inc.; Cogstate; Eisai

Inc.; Elan Pharmaceuticals, Inc.; Eli Lilly and Company; EuroImmun; F. Hoffmann-La Roche Ltd. and its affiliated company Genentech, Inc.; Fujirebio; GE Healthcare; IXICO Ltd.; Janssen Alzheimer Immunotherapy Research & Development, LLC.; Johnson & Johnson Pharmaceutical Research & Development LLC.; Lumosity; Lundbeck; Merck & Co., Inc.; Meso Scale Diagnostics, LLC.; NeuroRx Research; Neurotrack Technologies; Novartis Pharmaceuticals Corporation; Pfizer Inc.; Piramal Imaging; Servier; Takeda Pharmaceutical Company; and Transition Therapeutics. The Canadian Institutes of Health Research is providing funds to support ADNI clinical sites in Canada. Private sector contributions are facilitated by the Foundation for the National Institutes of Health (www.fnih.org). The grantee organization is the Northern California Institute for Research and Education, and the study is coordinated by the Alzheimer's Therapeutic Research Institute at the University of Southern California. ADNI data are disseminated by the Laboratory for Neuro Imaging at the University of Southern California.

FUNDING INFORMATION

This study was supported by the Nakayama Foundation for Human Science.

CONFLICT OF INTEREST

None of the authors declare any conflicts of interest.

DATA AVAILABILITY STATEMENT

Investigators may request access to anonymized data that were used in this study. Before using the data, proposals must be approved by the Institutional Review Boards at Tokyo Medical and Dental University Hospital.

ORCID

Qingmeng Chen  <https://orcid.org/0000-0002-1105-4835>

Takaaki Hattori  <https://orcid.org/0000-0002-4802-8606>

REFERENCES

- [Dataset] the Alzheimer's Disease Neuroimaging Initiative. (2003). the Alzheimer's Disease Neuroimaging Initiative (ADNI) database; DOD ADNI (Department of Defense award number W81XWH-12-2-0012).
- Ahmad, H., Taylor, B. V., van der Mei, I., Colman, S., O'Leary, B. A., Breslin, M., & Palmer, A. J. (2017). The impact of multiple sclerosis severity on health state utility values: Evidence from Australia. *Multiple Sclerosis*, 23(8), 1157–1166. <https://doi.org/10.1177/1352458516672014>
- Allali, G., Laidet, M., Assal, F., Chofflon, M., Armand, S., & Lalive, P. H. (2014). Dual-task assessment in natalizumab-treated multiple sclerosis patients. *European Neurology*, 71(5–6), 247–251. <https://doi.org/10.1159/000357217>
- Andersson, J. L. R., & Sotiropoulos, S. N. (2016). An integrated approach to correction for off-resonance effects and subject movement in diffusion MR imaging. *NeuroImage*, 125, 1063–1078. <https://doi.org/10.1016/j.neuroimage.2015.10.019>
- Awata, S., Sugiyama, M., Ito, K., Ura, C., Miyamae, F., Sakuma, N., Niikawa, H., Okamura, T., Inagaki, H., & Ijuin, M. (2016). Development of the dementia assessment sheet for community-based integrated care system. *Geriatrics & Gerontology International*, 16(Suppl 1), 123–131. <https://doi.org/10.1111/ggi.12727>

- Behrens, T. E., Berg, H. J., Jbabdi, S., Rushworth, M. F., & Woolrich, M. W. (2007). Probabilistic diffusion tractography with multiple fibre orientations: What can we gain? *NeuroImage*, 34(1), 144–155. <https://doi.org/10.1016/j.neuroimage.2006.09.018>
- Behrens, T. E., Woolrich, M. W., Jenkinson, M., Johansen-Berg, H., Nunes, R. G., Clare, S., Matthews, P. M., Brady, J. M., & Smith, S. M. (2003). Characterization and propagation of uncertainty in diffusion-weighted MR imaging. *Magnetic Resonance in Medicine*, 50(5), 1077–1088. <https://doi.org/10.1002/mrm.10609>
- Blumen, H. M., Holtzer, R., Brown, L. L., Gazes, Y., & Verghese, J. (2014). Behavioral and neural correlates of imagined walking and walking-while-talking in the elderly. *Human Brain Mapping*, 35(8), 4090–4104. <https://doi.org/10.1002/hbm.22461>
- Bonnet, M. C., Allard, M., Dilharreguy, B., Deloire, M., Petry, K. G., & Brochet, B. (2010). Cognitive compensation failure in multiple sclerosis. *Neurology*, 75(14), 1241–1248. <https://doi.org/10.1212/WNL.0b013e3181f612e3>
- Brandstadter, R., Ayeni, O., Krieger, S. C., Harel, N. Y., Escalon, M. X., Katz Sand, I., Leavitt, V. M., Fabian, M. T., Buyukturkoglu, K., Klineova, S., Riley, C. S., Lublin, F. D., Miller, A. E., & Sumowski, J. F. (2020). Detection of subtle gait disturbance and future fall risk in early multiple sclerosis. *Neurology*, 94(13), e1395–e1406. <https://doi.org/10.1212/wnl.0000000000008938>
- Brex, P. A., Ciccarelli, O., O'Riordan, J. I., Sailer, M., Thompson, A. J., & Miller, D. H. (2002). A longitudinal study of abnormalities on MRI and disability from multiple sclerosis. *The New England Journal of Medicine*, 346(3), 158–164. <https://doi.org/10.1056/NEJMoa011341>
- Brincks, J., Andersen, E. D., Sørensen, H., & Dalgas, U. (2017). Impaired postural balance correlates with complex walking performance in mildly disabled persons with multiple sclerosis. *NeuroRehabilitation*, 41(1), 227–235. <https://doi.org/10.3233/nre-171475>
- Bussas, M., Grahl, S., Pongratz, V., Berthele, A., Gasperi, C., Andlauer, T., Gaser, C., Kirschke, J. S., Wiestler, B., Zimmer, C., Hemmer, B., & Mühlau, M. (2022). Gray matter atrophy in relapsing-remitting multiple sclerosis is associated with white matter lesions in connecting fibers. *Multiple Sclerosis*, 28(6), 900–909. <https://doi.org/10.1177/13524585211044957>
- Cattaneo, D., Jonsdottir, J., & Coote, S. (2014). Targeting dynamic balance in falls-prevention interventions in multiple sclerosis: Recommendations from the international MS falls prevention research network. *International Journal of MS Care*, 16(4), 198–202. <https://doi.org/10.7224/1537-2073.2014-062>
- Corbetta, M., & Shulman, G. L. (2002). Control of goal-directed and stimulus-driven attention in the brain. *Nature Reviews Neuroscience*, 3(3), 201–215. <https://doi.org/10.1038/nrn755>
- Desikan, R. S., Ségonne, F., Fischl, B., Quinn, B. T., Dickerson, B. C., Blacker, D., Buckner, R. L., Dale, A. M., Maguire, R. P., Hyman, B. T., Albert, M. S., & Killiany, R. J. (2006). An automated labeling system for subdividing the human cerebral cortex on MRI scans into gyral based regions of interest. *NeuroImage*, 31(3), 968–980. <https://doi.org/10.1016/j.neuroimage.2006.01.021>
- Doi, T., Blumen, H. M., Verghese, J., Shimada, H., Makizako, H., Tsutsumimoto, K., Hotta, R., Nakakubo, S., & Suzuki, T. (2017). Gray matter volume and dual-task gait performance in mild cognitive impairment. *Brain Imaging and Behavior*, 11(3), 887–898. <https://doi.org/10.1007/s11682-016-9562-1>
- Dreher, J. C., & Grafman, J. (2003). Dissociating the roles of the rostral anterior cingulate and the lateral prefrontal cortices in performing two tasks simultaneously or successively. *Cerebral Cortex*, 13(4), 329–339. <https://doi.org/10.1093/cercor/13.4.329>
- Dujmovic, I., Radovanovic, S., Martinovic, V., Dackovic, J., Maric, G., Mesaros, S., Pekmezovic, T., Kostic, V., & Drulovic, J. (2017). Gait pattern in patients with different multiple sclerosis phenotypes. *Multiple Sclerosis and Related Disorders*, 13, 13–20. <https://doi.org/10.1016/j.msard.2017.01.012>
- Erickson, L. C., Rauschecker, J. P., & Turkeltaub, P. E. (2017). Meta-analytic connectivity modeling of the human superior temporal sulcus. *Brain Structure & Function*, 222(1), 267–285. <https://doi.org/10.1007/s00429-016-1215-z>
- Eshaghi, A., Marinescu, R. V., Young, A. L., Firth, N. C., Prados, F., Jorge Cardoso, M., Tur, C., De Angelis, F., Cawley, N., Brownlee, W. J., De Stefano, N., Laura Stromillo, M., Battaglini, M., Ruggieri, S., Gasperini, C., Filippi, M., Rocca, M. A., Rovira, A., Sastre-Garriga, J., ... Ciccarelli, O. (2018). Progression of regional grey matter atrophy in multiple sclerosis. *Brain*, 141(6), 1665–1677. <https://doi.org/10.1093/brain/awy088>
- Forsberg, A., Andreasson, M., & Nilsagård, Y. (2017). The functional gait assessment in people with multiple sclerosis: Validity and sensitivity to change. *International Journal of MS Care*, 19(2), 66–72. <https://doi.org/10.7224/1537-2073.2015-061>
- Fritz, N. E., Marasigan, R. E., Calabresi, P. A., Newsome, S. D., & Zackowski, K. M. (2015). The impact of dynamic balance measures on walking performance in multiple sclerosis. *Neurorehabilitation and Neural Repair*, 29(1), 62–69. <https://doi.org/10.1177/1545968314532835>
- Fujimori, J., Fujihara, K., Wattjes, M., & Nakashima, I. (2021). Patterns of cortical grey matter thickness reduction in multiple sclerosis. *Brain and Behavior: A Cognitive Neuroscience Perspective*, 11(4), e02050. <https://doi.org/10.1002/brb3.2050>
- Gonzales, J. U., Al-Khalil, K., & O'Boyle, M. (2019). Spatial task-related brain activity and its association with preferred and fast pace gait speed in older adults. *Neuroscience Letters*, 713, 134526. <https://doi.org/10.1016/j.neulet.2019.134526>
- Haider, L., Zrzavy, T., Hametner, S., Höftberger, R., Bagnato, F., Grabner, G., Trattnig, S., Pfeifenbring, S., Brück, W., & Lassmann, H. (2016). The topography of demyelination and neurodegeneration in the multiple sclerosis brain. *Brain*, 139(Pt 3), 807–815. <https://doi.org/10.1093/brain/awv398>
- Hamilton, F., Rochester, L., Paul, L., Rafferty, D., O'Leary, C. P., & Evans, J. J. (2009). Walking and talking: An investigation of cognitive-motor dual tasking in multiple sclerosis. *Multiple Sclerosis*, 15(10), 1215–1227. <https://doi.org/10.1177/1352458509106712>
- Hattori, T., Ito, K., Nakazawa, C., Numasawa, Y., Watanabe, M., Aoki, S., Mizusawa, H., Ishiai, S., & Yokota, T. (2018). Structural connectivity in spatial attention network: Reconstruction from left hemispatial neglect. *Brain Imaging and Behavior*, 12(2), 309–323. <https://doi.org/10.1007/s11682-017-9698-7>
- Hofer, S., & Frahm, J. (2006). Topography of the human corpus callosum revisited—Comprehensive fiber tractography using diffusion tensor magnetic resonance imaging. *NeuroImage*, 32(3), 989–994. <https://doi.org/10.1016/j.neuroimage.2006.05.044>
- Hua, K., Zhang, J., Wakana, S., Jiang, H., Li, X., Reich, D. S., Calabresi, P. A., Pekar, J. J., van Zijl, P. C., & Mori, S. (2008). Tract probability maps in stereotaxic spaces: Analyses of white matter anatomy and tract-specific quantification. *NeuroImage*, 39(1), 336–347. <https://doi.org/10.1016/j.neuroimage.2007.07.053>
- Ino, T., Usami, H., Tokumoto, K., Kimura, T., Ozawa, K., & Nakamura, S. (2008). Transient directional disorientation as a manifestation of cerebral ischemia. *European Neurology*, 60(1), 43–46. <https://doi.org/10.1159/000127979>
- Jahn, G., Wendt, J., Lotze, M., Papenmeier, F., & Huff, M. (2012). Brain activation during spatial updating and attentive tracking of moving targets. *Brain and Cognition*, 78(2), 105–113. <https://doi.org/10.1016/j.bandc.2011.12.001>
- Kalron, A., Dolev, M., & Givon, U. (2017). Further construct validity of the timed up-and-go test as a measure of ambulation in multiple sclerosis patients. *European Journal of Physical and Rehabilitation Medicine*, 53(6), 841–847. <https://doi.org/10.23736/s1973-9087.17.04599-3>
- Kucyi, A., Hodaie, M., & Davis, K. D. (2012). Lateralization in intrinsic functional connectivity of the temporoparietal junction with salience- and

- attention-related brain networks. *Journal of Neurophysiology*, 108(12), 3382–3392. <https://doi.org/10.1152/jn.00674.2012>
- Kurtzke, J. F. (1983). Rating neurologic impairment in multiple sclerosis: An expanded disability status scale (EDSS). *Neurology*, 33(11), 1444–1452. <https://doi.org/10.1212/wnl.33.11.1444>
- Lizrova Preiningerova, J., Novotna, K., Ruzs, J., Sucha, L., Ruzicka, E., & Havrdova, E. (2015). Spatial and temporal characteristics of gait as outcome measures in multiple sclerosis (EDSS 0 to 6.5). *Journal of Neuroengineering and Rehabilitation*, 12, 14. <https://doi.org/10.1186/s12984-015-0001-0>
- Logie, R. H., Cocchini, G., Delia Sala, S., & Baddeley, A. D. (2004). Is there a specific executive capacity for dual task coordination? Evidence from Alzheimer's disease. *Neuropsychology*, 18(3), 504–513. <https://doi.org/10.1037/0894-4105.18.3.504>
- Lorefice, L., Coghe, G., Fenu, G., Porta, M., Pilloni, G., Frau, J., Corona, F., Sechi, V., Barracchi, M. A., Marrosu, M. G., Pau, M., & Cocco, E. (2017). 'Timed up and go' and brain atrophy: A preliminary MRI study to assess functional mobility performance in multiple sclerosis. *Journal of Neurology*, 264(11), 2201–2204. <https://doi.org/10.1007/s00415-017-8612-y>
- Marek, S., & Dosenbach, N. U. F. (2018). The frontoparietal network: Function, electrophysiology, and importance of individual precision mapping. *Dialogues in Clinical Neuroscience*, 20(2), 133–140. <https://doi.org/10.31887/DCNS.2018.20.2/smarek>
- Martin, C. L., Phillips, B. A., Kilpatrick, T. J., Butzkueven, H., Tubridy, N., McDonald, E., & Galea, M. P. (2006). Gait and balance impairment in early multiple sclerosis in the absence of clinical disability. *Multiple Sclerosis*, 12(5), 620–628. <https://doi.org/10.1177/1352458506070658>
- Muto, T., Herzberger, B., Hermsdoerfer, J., Miyake, Y., & Poepfel, E. (2012). Interactive cueing with Walk-Mate for hemiparetic stroke rehabilitation. *Journal of Neuroengineering and Rehabilitation*, 9, 58. <https://doi.org/10.1186/1743-0003-9-58>
- Nasreddine, Z. S., Phillips, N. A., Bédirian, V., Charbonneau, S., Whitehead, V., Collin, I., Cummings, J. L., & Chertkow, H. (2005). The Montreal cognitive assessment, MoCA: A brief screening tool for mild cognitive impairment. *Journal of the American Geriatrics Society*, 53(4), 695–699. <https://doi.org/10.1111/j.1532-5415.2005.53221.x>
- O'Connell, M. A., & Basak, C. (2018). Effects of task complexity and age-differences on task-related functional connectivity of attentional networks. *Neuropsychologia*, 114, 50–64. <https://doi.org/10.1016/j.neuropsychologia.2018.04.013>
- Pareto, D., Sastre-Garriga, J., Aymerich, F. X., Auger, C., Tintoré, M., Montalban, X., & Rovira, A. (2016). Lesion filling effect in regional brain volume estimations: A study in multiple sclerosis patients with low lesion load. *Neuroradiology*, 58(5), 467–474. <https://doi.org/10.1007/s00234-016-1654-5>
- Peterson, D. S., Gera, G., Horak, F. B., & Fling, B. W. (2017). Corpus callosum structural integrity is associated with postural control improvement in persons with multiple sclerosis who have minimal disability. *Neurorehabilitation and Neural Repair*, 31(4), 343–353. <https://doi.org/10.1177/1545968316680487>
- Raichle, M. E., MacLeod, A. M., Snyder, A. Z., Powers, W. J., Gusnard, D. A., & Shulman, G. L. (2001). A default mode of brain function. *Proceedings of the National Academy of Sciences of the United States of America*, 98(2), 676–682. <https://doi.org/10.1073/pnas.98.2.676>
- Rocca, M. A., Gallo, A., Colombo, B., Falini, A., Scotti, G., Comi, G., & Filippi, M. (2004). Pyramidal tract lesions and movement-associated cortical recruitment in patients with MS. *NeuroImage*, 23(1), 141–147. <https://doi.org/10.1016/j.neuroimage.2004.05.005>
- Rotstein, D. L., Healy, B. C., Malik, M. T., Chitnis, T., & Weiner, H. L. (2015). Evaluation of no evidence of disease activity in a 7-year longitudinal multiple sclerosis cohort. *JAMA Neurology*, 72(2), 152–158. <https://doi.org/10.1001/jamaneurol.2014.3537>
- Schmidt, E. L., Burge, W., Visscher, K. M., & Ross, L. A. (2016). Cortical thickness in frontoparietal and cingulo-opercular networks predicts executive function performance in older adults. *Neuropsychology*, 30(3), 322–331. <https://doi.org/10.1037/neu0000242>
- Schmidt, P., Gaser, C., Arsic, M., Buck, D., Förschler, A., Berthele, A., Hoshi, M., Ilg, R., Schmid, V. J., Zimmer, C., Hemmer, B., & Mühlau, M. (2012). An automated tool for detection of FLAIR-hyperintense white-matter lesions in multiple sclerosis. *NeuroImage*, 59(4), 3774–3783. <https://doi.org/10.1016/j.neuroimage.2011.11.032>
- Sliwinska, M. W., Elson, R., & Pitcher, D. (2020). Dual-site TMS demonstrates causal functional connectivity between the left and right posterior temporal sulci during facial expression recognition. *Brain Stimulation*, 13(4), 1008–1013. <https://doi.org/10.1016/j.brs.2020.04.011>
- Smith, S. M., Jenkinson, M., Johansen-Berg, H., Rueckert, D., Nichols, T. E., Mackay, C. E., Watkins, K. E., Ciccarelli, O., Cader, M. Z., Matthews, P. M., & Behrens, T. E. (2006). Tract-based spatial statistics: Voxelwise analysis of multi-subject diffusion data. *NeuroImage*, 31(4), 1487–1505. <https://doi.org/10.1016/j.neuroimage.2006.02.024>
- Smith, S. M., Jenkinson, M., Woolrich, M. W., Beckmann, C. F., Behrens, T. E., Johansen-Berg, H., Bannister, P. R., De Luca, M., Drobnjak, I., Flitney, D. E., Niazy, R. K., Saunders, J., Vickers, J., Zhang, Y., De Stefano, N., Brady, J. M., & Matthews, P. M. (2004). Advances in functional and structural MR image analysis and implementation as FSL. *NeuroImage*, 23(Suppl 1), S208–S219. <https://doi.org/10.1016/j.neuroimage.2004.07.051>
- Sormani, M. P., & De Stefano, N. (2013). Defining and scoring response to IFN-beta in multiple sclerosis. *Nature Reviews. Neurology*, 9(9), 504–512. <https://doi.org/10.1038/nrneurol.2013.146>
- Sormani, M. P., Rio, J., Tintore, M., Signori, A., Li, D., Cornelisse, P., Stubinski, B., Stromillo, M., Montalban, X., & De Stefano, N. (2013). Scoring treatment response in patients with relapsing multiple sclerosis. *Multiple Sclerosis*, 19(5), 605–612. <https://doi.org/10.1177/1352458512460605>
- Spain, R. I., St George, R. J., Salarian, A., Mancini, M., Wagner, J. M., Horak, F. B., & Bourdette, D. (2012). Body-worn motion sensors detect balance and gait deficits in people with multiple sclerosis who have normal walking speed. *Gait & Posture*, 35(4), 573–578. <https://doi.org/10.1016/j.gaitpost.2011.11.026>
- Strik, M., Cofré Lizama, L. E., Shanahan, C. J., van der Walt, A., Boonstra, F. M. C., Glarin, R., Kilpatrick, T. J., Geurts, J. J. G., Cleary, J. O., Schoonheim, M. M., Galea, M. P., & Kolbe, S. C. (2021). Axonal loss in major sensorimotor tracts is associated with impaired motor performance in minimally disabled multiple sclerosis patients. *Brain Communication*, 3(2), fcab032. <https://doi.org/10.1093/braincomms/fcab032>
- Takakusaki, K. (2017). Functional neuroanatomy for posture and gait control. *Journal of Movement Disorders*, 10(1), 1–17. <https://doi.org/10.14802/jmd.16062>
- Tanglay, O., Young, I. M., Dadario, N. B., Briggs, R. G., Fonseka, R. D., Dhanaraj, V., Hormovas, J., Lin, Y. H., & Sughrue, M. E. (2022). Anatomy and white-matter connections of the precuneus. *Brain Imaging and Behavior*, 16(2), 574–586. <https://doi.org/10.1007/s11682-021-00529-1>
- Thompson, A. J., Banwell, B. L., Barkhof, F., Carroll, W. M., Coetzee, T., Comi, G., Correale, J., Fazekas, F., Filippi, M., Freedman, M. S., Fujihara, K., Galetta, S. L., Hartung, H. P., Kappos, L., Lublin, F. D., Marrie, R. A., Miller, A. E., Miller, D. H., Montalban, X., ... Cohen, J. A. (2018). Diagnosis of multiple sclerosis: 2017 revisions of the McDonald criteria. *The Lancet Neurology*, 17(2), 162–173. [https://doi.org/10.1016/s1474-4422\(17\)30470-2](https://doi.org/10.1016/s1474-4422(17)30470-2)
- Tomblin, M., & Jolicoeur, P. (2003). A central capacity sharing model of dual-task performance. *Journal of Experimental Psychology. Human Perception and Performance*, 29(1), 3–18. <https://doi.org/10.1037/0096-1523.29.1.3>
- Tripathi, S., Verghese, J., & Blumen, H. M. (2019). Gray matter volume covariance networks associated with dual-task cost during walking-

- while-talking. *Human Brain Mapping*, 40(7), 2229–2240. <https://doi.org/10.1002/hbm.24520>
- Utevsky, A. V., Smith, D. V., & Huettel, S. A. (2014). Precuneus is a functional core of the default-mode network. *The Journal of Neuroscience*, 34(3), 932–940. <https://doi.org/10.1523/jneurosci.4227-13.2014>
- Weinshenker, B. G., Rice, G. P., Noseworthy, J. H., Carriere, W., Baskerville, J., & Ebers, G. C. (1991). The natural history of multiple sclerosis: A geographically based study. 3. Multivariate analysis of predictive factors and models of outcome. *Brain*, 114(Pt 2), 1045–1056. <https://doi.org/10.1093/brain/114.2.1045>
- Yeo, B. T., Krienen, F. M., Sepulcre, J., Sabuncu, M. R., Lashkari, D., Hollinshead, M., Roffman, J. L., Smoller, J. W., Zöllei, L., Polimeni, J. R., Fischl, B., Liu, H., & Buckner, R. L. (2011). The organization of the human cerebral cortex estimated by intrinsic functional connectivity. *Journal of Neurophysiology*, 106(3), 1125–1165. <https://doi.org/10.1152/jn.00338.2011>
- Ziemssen, T., Derfuss, T., de Stefano, N., Giovannoni, G., Palavra, F., Tomic, D., Vollmer, T., & Schippling, S. (2016). Optimizing treatment success in multiple sclerosis. *Journal of Neurology*, 263(6), 1053–1065. <https://doi.org/10.1007/s00415-015-7986-y>

SUPPORTING INFORMATION

Additional supporting information can be found online in the Supporting Information section at the end of this article.

How to cite this article: Chen, Q., Hattori, T., Tomisato, H., Ohara, M., Hirata, K., Yokota, T., & for the Alzheimer's Disease Neuroimaging Initiative (2023). Turning and multitask gait unmask gait disturbance in mild-to-moderate multiple sclerosis: Underlying specific cortical thinning and connecting fibers damage. *Human Brain Mapping*, 44(3), 1193–1208. <https://doi.org/10.1002/hbm.26151>